Published November 1, 1998

Mechanism of Peptide-induced Mast Cell Degranulation
Translocation and Patch-Clamp Studies

Dorothea Lorenz,* Burkhard Wiesner,* Josef Zipper,* Anett Winkler,* Eberhard Krause,* Michael Beyermann,* Manfred Lindau,‡ and Michael Bienert*

From the *Institute of Molecular Pharmacology, 10315 Berlin, Germany; and ‡School of Applied and Engineering Physics, Cornell University, Ithaca, New York 14853-2501

ABSTRACT Substance *P* and other polycationic peptides are thought to stimulate mast cell degranulation via direct activation of G proteins. We investigated the ability of extracellularly applied substance *P* to translocate into mast cells and the ability of intracellularly applied substance *P* to stimulate degranulation. In addition, we studied by reverse transcription–PCR whether substance *P*-specific receptors are present in the mast cell membrane. To study translocation, a biologically active and enzymatically stable fluorescent analogue of substance *P* was synthesized. A rapid, substance *P* receptor- and energy-independent uptake of this peptide into pertussis toxin-treated and -untreated mast cells was demonstrated using confocal laser scanning microscopy. The peptide was shown to localize preferentially on or inside the mast cell granules using electron microscopic autoradiography with ^{125}I-labeled all-D substance *P* and ^{3}H-labeled substance *P*. Cell membrane capacitance measurements using the patch-clamp technique demonstrated that intracellularly applied substance *P* induced calcium transients and activated mast cell exocytosis with a time delay that depended on peptide concentration (delay of 100–500 s at concentrations of substance *P* from 50 to 5 μM). Degranulation in response to intracellularly applied substance *P* was inhibited by GDPβS and pertussis toxin, suggesting that substance *P* acts via G protein activation. These results support the recently proposed model of a receptor-independent mechanism of peptide-induced mast cell degranulation, which assumes a direct interaction of peptides with G protein α subunits subsequent to their translocation across the plasma membrane.

KEY WORDS: substance *P* • exocytosis • confocal laser scanning microscopy • electron microscopy • capacitance

INTRODUCTION

Mast cells stimulated with immunoglobulin E/antigen release a variety of preformed mediators (e.g., histamine) by exocytosis. They can, however, also be triggered to undergo exocytosis by nonantigenic stimuli. Polycationic substances, such as the neuropeptides substance *P* (SP)[1] (Repke and Bienert, 1987) or neuropeptide Y (Gundemar and Håkanson, 1991), or the venom peptides mastoparan and mast cell degranulating peptide (Mousli et al., 1989; Landry et al., 1992), and naturally occurring or synthetic polyamines such as spermine (Purcell et al., 1996) and compound 48/80 (Paton, 1951) stimulate the release of vasoactive and inflammatory compounds from mast cells. The peptidergic stimulation of mast cells has raised the question of whether other peptide-secreting cells in the vicinity of mast cells are capable of stimulating mast cells. In this context, it is interesting to note that mast cells have been found in close proximity to peptidergic neurones, suggesting a probable functional relationship between the immune and nervous systems (McKay and Bienenstock, 1994; Marshall and Waserman, 1995; Purcell and Atterwill, 1995) mediated by neuropeptides.

The mechanism by which cationic peptides and polyamines stimulate mast cell exocytosis remains unclear. It is generally accepted that heterotrimeric GTP-binding proteins (G proteins) are involved in the stimulation of mast cell degranulation by basic secretagogues. Thus, application of substance *P* and other cationic secretagogues transiently increases intracellular Ca^{2+} concentrations through G protein-mediated activation of phospholipase C (PLC), and pretreatment of mast cells with pertussis toxin abolishes both inositol-3-phosphate production and peptide-induced mast cell de-

Anett Winkler's present address is Addiction Research Group, Max-Planck-Institute for Psychiatry, Kraepelin-Strasse 2, D-80804 München, Germany.

Address correspondence to Dr. Dorothea Lorenz, Abt. Signaltransduktion/Molekulare Medizin, Forschungsinstitut für Molekulare Pharmakologie, Alfred-Kowalke-Strasse 4, D-10315 Berlin, Germany. Fax: 030 51 5 51 333; E-mail: lorenz@fmp-berlin.de

[1]*Abbreviations used in this paper:* ^{3}H-SP, ^{3}H-labeled SP; all-D-SP, D-amino acid analogue of SP; CLSM, confocal laser scanning microscopy; C_m, membrane capacitance; ES, external bath solution; FLUOS-SP, 5(6)-carboxyfluorescein-labeled Arg^{3},Orn^{7}-SP; FLUOS-all-D-SP, 5(6)-carboxyfluorescein-labeled all-D-Arg^{3},Orn^{7}-SP; GAPDH, glyceraldehyde-phosphate dehydrogenase; IS, intracellular or pipette solution; PLC, phospholipase C; PtX, pertussis toxin; ROI, region of interest; R_s, series resistance; RT-PCR, reverse transcription–PCR; SP, substance *P*.

Published November 1, 1998

granulation (Mousli et al., 1989, 1995; Emadi-Khiav et al., 1995). Experiments with permeabilized (Cockcroft et al., 1987; Aridor et al., 1990; Lillie and Gomperts, 1992) and patch-clamped (Lindau and Nüße, 1987; Penner, 1988) mast cells and neutrophils (Nüße and Lindau, 1990) have demonstrated the involvement of a G protein downstream of PLC capable of inducing exocytosis. A recently identified heterotrimeric G protein (G_{i3}) on the plasma membrane of mast cells (Aridor et al., 1993) is thought to participate in the control of one of the late steps of exocytosis. Furthermore, cationic peptides stimulate purified and reconstituted G_i/G_o proteins from calf brain (Higashijima et al., 1990; Mousli et al., 1990*a*, 1995) and G proteins from rat peritoneal mast cells (Bueb et al., 1990; Fischer et al., 1993). However, the presence of specific peptide receptors in the mast cell membrane is questionable. Peptide concentrations in the micromolar range are necessary to induce mast cell degranulation and both studies of structure–activity relationships and receptor autoradiography failed to detect specific peptide receptors on mast cells (Repke and Bienert, 1987; Repke et al., 1987; O'Flynn et al., 1989; Mousli et al., 1994). In view of these difficulties, Mousli et al. (1990*b*) proposed a direct interaction of cationic peptides with heterotrimeric G proteins without the participation of a receptor. This process would require insertion into and translocation of peptides across the plasma membrane. In previous studies it was also proposed that the initial event in peptide-induced mast cell stimulation might be an interaction of the cationic peptides with negatively charged sites (e.g., sialic acid containing glycoproteins) at the mast cell membrane (Mousli et al., 1990*b*, Emadi-Khiav et al., 1995). In contrast to the requirements for the activation of purified G_i proteins by mastoparan-peptides, amphipathic helicity was proposed to be not obligatory for peptide-induced mast cell activation (Cross et al., 1995). Nevertheless, these investigations do not exclude the possibility of a direct interaction of exogenous peptides with G proteins after their binding to glycoproteins and subsequent transport across the plasma membrane into the cell.

The aim of the present investigation was to clarify whether a transport of cationic peptides into rat peritoneal mast cells is possible and whether intracellularly applied peptide can induce mast cell degranulation. The transport studies were performed by confocal laser scanning microscopy using fluorescence-labeled Arg^3, Orn^7-SP (FLUOS-SP) and its D-amino acid analogue, all-D-Arg^3,Orn^7-SP (FLUOS-all-D-SP), as well as by electron microscopic autoradiography using ^{3}H-labeled SP and ^{125}I-labeled all-D-SP. The action of intracellularly applied peptide on mast cell degranulation was studied by cell membrane capacitance measurements using the patch-clamp technique in the whole-cell configuration. Additionally, in search of SP-specific receptors in rat peritoneal mast cells, reverse transcription–PCR (RT-PCR) was used.

The results of our investigations demonstrate that SP peptides can be rapidly and energy-independently translocated into mast cells. By electron microscopic studies, an exclusively granule-related intracellular location of SP was confirmed. Moreover, intracellularly applied peptide was shown to induce mast cell activation. In addition, SP receptor-specific mRNA was not detected. These results support the concept of a receptor-independent but receptor-mimicking action of SP when mast cells are exposed to micromolar concentrations of SP in vitro.

MATERIALS AND METHODS

Reagents

Unless otherwise noted, all reagents and chemicals were purchased from Sigma Chemical Co. (Deisenhofen, Germany).

Peptide Synthesis and Fluorescence Labeling of Peptides

Substance *P* (H-Arg-Pro-Lys-Pro-Gln-Gln-Phe-Phe-Gly-Leu-MetNH_2) and its D-amino acid analogue all-D-SP were synthesized by solid-phase method using standard Fmoc chemistry and purified (purity > 95%) as described (Cross et al., 1995). For fluorescence labeling, 5.6 μmol H-Arg-Pro-Arg-Pro-Gln-Gln-Phe-Orn-Gly-Leu-MetNH_2 (Arg^3,Orn^7-SP) or the corresponding all-D-peptide, respectively, were dissolved in 3.3 ml 0.1 M borate buffer (pH 9.0) and 4.7 μmol 5(6)-carboxyfluorescein-*N*′-hydroxysuccinimide ester (FLUOS; Boehringer Mannheim, Mannheim, Germany) dissolved in 0.8 ml acetonitrile was added. The reaction mixture was incubated at 25°C for 15 min in the dark. Under these conditions, the labeling occurs selectively at the N^ε-amino group of Orn. The FLUOS peptides were purified by semipreparative HPLC (purity > 95%).

Mast Cell Preparation

Peritoneal mast cells were obtained from male Wistar rats (300–350 g) by peritoneal lavage with incubation medium containing (mM): 112 NaCl, 4 KCl, 1 $MgCl_2$, 1.6 $CaCl_2$, 8 HEPES, 6.7 glucose, 36 $NaHCO_3$, 0.32 KH_2PO_4, 2.2 HCl, pH 7.3, 300 mOsm/kg. After centrifugation (150 *g*, 5 min) and resuspension of the pellet in 2 ml HEPES buffer containing (mM): 135 NaCl, 2.7 KCl, 1.8 $CaCl_2$, 1 $MgCl_2$, 20 HEPES, 5.6 glucose, 1 mg/ml bovine serum albumin, pH 7.3, 300 mOsm/kg, cells were purified by centrifugation through 2 ml isotonic Percoll (Pharmacia Fine Chemicals, Uppsala, Sweden) (75%) at 200 *g* for 15 min, washed and centrifuged twice at 100 *g* for 5 min in HEPES buffer. Cells were subsequently resuspended either in external solution (ES) (containing [mM]: 140 NaCl, 5 KCl, 2 $CaCl_2$, 1 $MgCl_2$, 10 HEPES, 15 glucose, pH 7.2, 300 mOsm/kg) for transport experiments or in Dulbecco's modified Eagle medium (nutrient mixture F-12 HAM) supplemented with 2 mM glutamine and incubated in a humidified atmosphere with 5% CO_2 and 95% air at 37°C before use in patch-clamp experiments. The cell purity and viability were tested by toluidine blue staining and trypan blue exclusion (both > 95%), respectively.

Published November 1, 1998

Pertussis Toxin Treatment

To prevent degranulation during the transport experiments and in some patch-clamp experiments, mast cells were pretreated with 200 ng/ml pertussis toxin (PtX) for 2 h or with 1 μg/ml for up to 9 h, respectively, at 37°C in a humidified atmosphere with 5% CO_2 and 95% air.

Histamine Release

Histamine release was quantified as described previously (Cross et al., 1993). In brief, an aliquot of rat peritoneal mast cells in ES was incubated with an aliquot of peptide solution for 10 min at 37°C. The reaction was quenched by adding ice cold ES, the suspension was centrifuged at 200 *g* for 5 min and the supernatant removed for histamine assay. The total amount of histamine was determined from control samples after incubation in a boiling water bath for 5 min. The histamine assay was performed as described by Repke et al. (1987).

Release was expressed as a percentage of the total histamine content of the cells and was corrected for the spontaneous release occurring in the absence of any stimuli.

Translocation Experiments

Confocal laser scanning microscopy. For the investigation of translocation of SP across the plasma membrane into the cytoplasm of mast cells, FLUOS-SP and FLUOS-all-D-SP were used. The reason for using the D-amino acid analogue of SP is its resistance to enzymatic degradation compared with SP. High performance liquid chromatographic studies showed that SP was degraded in mast cell suspension and in supernatants of mast cell suspensions within 30 min of incubation, whereas all-D-SP was not degraded even after 1 h of incubation (D. Lorenz, unpublished results). To prevent degranulation-induced artifacts during the transport experiments, mast cells were pretreated with PtX.

Three series of experiments were performed.

(*a*) Purified PtX-treated mast cells were incubated with 30 μM peptide solution in ES for 1–32 min at room temperature and washed three times (centrifugation at 100 *g*, 20 min) in 9 ml ice cold ES supplemented with 6 mM $CaCl_2$ and 1% bovine serum albumin to remove extracellular peptide. The cell pellets were resuspended in 200 μl ES and allowed to adhere to the glass base of a culture dish. The intracellular fluorescence intensity from the central optical section of single mast cells was then monitored.

(*b*) 200 μl of a 2.5-μM peptide solution were added via a 1-ml syringe to 200 μl of ES in a dish containing adherent mast cells. The time courses of the fluorescence intensities inside and outside the cell in predetermined regions of interest (ROIs, 16 × 16 pixel) were simultaneously recorded at a frequency of 0.2 Hz for up to 30 min. The background fluorescence intensity was determined before the addition of the peptide solution for 300 s. Due to the strong extracellular fluorescence intensity, the intracellular signal was superimposed to some extent by extracellular fluorescence arising from the nonideal confocal properties of the confocal laser scanning microscopy (CLSM). The intracellular fluorescence signal was corrected for this contribution by estimating the distribution function of the sensitivity in the z direction of the microscope, as described elsewhere (Wiesner, Lorenz, Krause, Baeger, Beyermann, and Bienert, manuscript in preparation).

(*c*) 100 μl of solutions containing different peptide concentrations were mixed with 100 μl of mast cell suspension 5 min before measurements. The cells were allowed to adhere and the fluorescence intensities of ROIs inside and outside the cell were measured (30 scans with a scan time of 2 s with double averaging). All intensities were corrected for the small contribution from extracellular out-of-focus-fluorescence as described. For measurements with metabolically inhibited cells, the cells in ES without glucose were treated with 1 μM antimycin for 20 min at 37°C or with 33 μM dinitrophenol for 10 min at room temperature before the addition of the peptide solution. Additionally, antimycin was added simultaneously with the peptide solution and the suspensions were subsequently incubated for the given times.

After each measurement, 100 μl of 0.5% trypan blue were added to the cells and the trypan blue fluorescence (λexc = 543 nm, λem > 590 nm) was monitored to confirm the integrity of the plasma membrane.

For all translocation studies, we used the confocal laser scanning microscope LSM 410 Invert (Carl Zeiss Jena GmbH, Jena, Germany) with an excitation Argon-Krypton laser (488 nm) and a Helium-Neon laser (543 nm). The laser beam was focused with a ×63/1.25 oil immersion objective (Plan-Neofluar; Carl Zeiss Jena GmbH). The fluorescence light passed through a dichroic mirror (FT 510 at excitation 488 nm, NT 543/80/20 at excitation 543 nm, both from Carl Zeiss Jena GmbH) and an additional cut-off-filter (LP 515 at excitation 488 nm and LP 590 at excitation 543 nm, both from Carl Zeiss Jena GmbH) in front of the photomultiplier.

The data were expressed as mean ± SD.

Electron Microscopic Autoradiography

For these experiments, ^{3}H-labeled SP (^{3}H-SP) ([2-prolyl-3,4-^{3}H(N)]-SP, specific activity 1,147 GBq/mmol, 37 MBq/ml; DuPont/NEN, Bad Homburg, Germany) and ^{125}I-labeled all-D-SP (^{125}I-all-D-SP) (^{125}I labeling of all-D-SP on Lys via the Bulton-Hunter reaction by [DuPont/NEN]: specific activity 81,400 GBq/mmol, 7.4 MBq/ml) were used. The radio-chemical purity was determined before the experiments by radioactive HPLC and was found to be 98.4 and 95.6% for ^{3}H-SP and ^{125}I-all-D-SP, respectively (HPLC-system; JASCO, Tokyo, Japan, radioactivity HPLC-monitor RAMONA 93; RAYTEST, Straubenhardt, Germany, HPLC column (250 × 4 mm), and precolumn LiChrospher 100 RP-18, 5 μm endcapped; Merck, Darmstadt, Germany, mobile phase: 30% acetonitrile/70% aqueous-0.2% trifluoroacetic acid).

Pooled, purified, PtX-treated, and washed, cells were incubated for 10 min at room temperature with 1.5 ml ^{3}H-SP solution in ES (1.8 MBq; final volume of cell suspension, 1.6 ml; peptide concentration, 1 μM) and for 10 and 60 min with 1.0 ml ^{125}I-all-D-SP solution (0.18 MBq; final volume of cell suspension, 1.1 ml; peptide concentration, 2 nM). In control experiments, cells were incubated with SP or all-D-SP solutions with the same concentration of unlabeled peptide. After centrifugation (200 *g*, 2 min) and washing twice with ES and subsequently with phosphate buffer (0.1 M, pH 7.4, 290 mOsm/kg), the resuspended cells were fixed in phosphate-buffered 3% glutaraldehyde with continuous shaking for 1 h at room temperature. Post-fixation with osmium tetroxide was omitted to prevent dislocation and/or loss of SP cross-linked with cellular proteins by glutaraldehyde. After careful rinses (six times) with phosphate buffer, mast cells were solidly pelleted in the presence of low gel point agarose (2%). These tissue-like specimens were, after microdissection, dehydrated by graded concentrations of ethanol, embedded in Epon 812, and sectioned with an Ultracut S (REICHERT, Vienna, Austria).

The ultrathin sections were coated with monocrystalline layers of ILFORD Nuclear Research Emulsion L 4 (ILFORD PHOTO Co., London, UK). After exposure for 12 wk (4°C), autoradiographs were developed (KODAK D 19; Eastman Kodak Co., Rochester, NY) and investigated using a ZEISS 902 A electron microscope (Carl Zeiss Jena GmbH) at 80 kV.

Published November 1, 1998

In addition to electron microscopic autoradiography, the uptake of SP was also examined autoradiographically on native mast cells. For this purpose, PtX- and SP-treated washed (once ES, once phosphate buffer) cells were resuspended in a small volume of phosphate-buffered 20% polyvinylpyrrolidone (K30) solution (as cryoprotectant) and transferred into channels (2 mm diameter, 4 mm deep) punched into slices of unfixed liver tissue. These specimens were shock frozen on an aluminium block (80 mm diameter, 250 mm high) and placed in liquid nitrogen. After storage at −80°C for some days, the mast cells "embedded" in liver tissue were sectioned (5 μm) with a cryostat (LEICA/Jung CM 3000; Leica Inc., Deerfield, IL), mounted on poly-L-lysine coated slides, air dried, and dipped in ILFORD nuclear Research Emulsion L 4 (diluted 1:1). Exposure at 4°C with desiccant for 4 wk was followed by development of autoradiographs with KODAK D 19 (1:1), staining with neutral red and investigation using a LEITZ microscope DIAPLAN (Leica Mikroskopie und Systeme GmbH, Wetzlar, Germany).

Patch-Clamp Measurements

The action of intracellularly applied SP on degranulation was monitored by measurements of cell membrane capacitance using the patch-clamp technique. Experiments were performed in a tight seal whole-cell voltage-clamp at room temperature. Data were collected with an EPC-9 amplifier (HEKA elektronik, Lambrecht, Germany) using HEKA-software PULSE and X-CHART run on a Macintosh Quadra 650 computer. Membrane capacitance (C_m) and series resistance (R_s) were measured automatically by the EPC-9 "cap.track" feature, based on the "time domain" technique (Lindau and Neher, 1988) and the use of an algorithm described by Sigworth et al. (1995). This technique has been shown to produce equivalent values of C_m to those obtained with the "frequency domain" method (Neher and Zucker, 1993). The filters were set by the software automatically; the amplitude of the square-wave voltage pulses was set to 5 mV, and 15 cycles were used for C_m and R_s estimates. The frequency for C_m and R_s determination was 3–4 Hz. Membrane resistance (R_m) was obtained by subtracting R_s from the quantity R_m displayed in the EPC-9 window. Holding potential was set to 0 mV. No corrections were made for liquid junction potential, which was determined to be 8.3 mV for the bath and pipette solution used. In parallel with capacitance measurements, the degranulation was monitored by a video camera mounted on the microscope (ZEISS AXIOVERT TV 135; Carl Zeiss Jena GmbH) equipped with Nomarski optics.

Sylgard-coated borosilicate glass pipettes (Hilgenberg, Malsfeld, Germany) were used (electrode resistance 2.5–5 MΩ when filled with the intracellular pipette solution). In the experiments with dialyzed peptide, R_s varied between 10 and 80 MΩ and membrane conductance (G_m) between 0.2 and 5 nS. For evaluation of the data, only cells with $R_s < 50$ MΩ and $G_m < 2$ nS were considered.

Bath solution ES contained (mM): 140 NaCl, 5 KCl, 2 $CaCl_2$, 1 $MgCl_2$, 10 HEPES, 15–20 mM glucose, pH 7.2, 300 mOsm/kg).

Pipette solution (IS) 1 contained (mM): 135 K-glutamate, 10 NaCl, 7 $MgCl_2$, 10 HEPES, 0.5 MgATP, pH 7.2, 290 mOsm/kg. EGTA, GTPγS (Boehringer Mannheim), and SP were added at the desired concentration as indicated in the figures. IS 2 was of the same composition as IS 1 but with 20 mM NaCl and 1 mM $MgCl_2$.

Degranulation measured as increase of capacitance in patch-clamped mast cells started after a delay after patch rupture and peptide diffusion into the cell. Thereafter, the degranulation proceeded for several minutes and the capacitance approached a final value. For comparison of different cells, the time delay was defined as that time at which the capacitance increased by 10% of the initial value; the rate of degranulation was obtained from the average slope of the curve between 10 and 90% of the degranulation amplitude.

Measurement of diffusion of the peptide from the pipette into the cell using FLUOS-all-D-SP was performed using previously described equipment for patch-clamp and fluorescence measurements (Nüße and Lindau, 1990) and also using the Ca^{2+}-imaging IONVISION system (Improvision, Coventry, UK) coupled to the patch-clamp set-up using an extended ISIS Intensified CCD-camera (Photonics Science, Millham, UK), the polychromatic illumination system (TILL photonics, Munich, Germany) at excitation wavelength 488 nm, FLUAR ×100/1.3 oil immersion objective (Carl Zeiss Jena GmbH) and dichroic mirror FT 510, as well as a cut-off filter LP 520 (both Carl Zeiss Jena GmbH) in the AXIOVERT TV135 microscope and the IONVISION software.

Intracellular free Ca^{2+} concentrations $[Ca^{2+}]_i$ in patch-clamped mast cells were determined in parallel with C_m measurements with 100 μM FURA-2 (Molecular Probes, Inc., Eugene, OR) loaded into the cells by diffusion from the recording pipette. Fluorescence images (using a dichroic mirror Zeiss FT 425 and an interference filter Zeiss IF 500–530 in front of the CCD camera) were captured by alternately exciting FURA-2 in the cells at 340 nm (image A) and 380 nm (image B). Background images were captured in the cell-attached configuration before patch rupture. After background subtraction, the ratioing of the images (A/B) was performed off-line and converted on a pixel by pixel basis to an image that represented the variable ion concentration within the cell. For calibration of the system, mast cells were patched with IS 2 containing 100 μM FURA-2 and Ca^{2+} buffers with known concentrations of free Ca^{2+} (10 mM EGTA supplemented to the appropriate $CaCl_2$ concentrations prepared using the concentrated Ca^{2+} buffering kit from Molecular Probes, Inc.), and the fluorescence images from 340 and 380 nm excitation were recorded. The ratio of fluorescence intensity (grey levels) inside the cell at the two excitation wavelengths was calculated after background subtraction from the two images. Using IONVISION software, a calibration curve (ratio versus $[Ca^{2+}]_i$) was derived and used for the determination of free Ca^{2+} concentration inside the cell. Images were captured by averaging two frames. Dual image acquisition was performed every 1.66 s.

The data from patch-clamp measurements were expressed as mean ± SEM (number of cells).

PCR Experiments

Total RNA was isolated from purified peritoneal rat mast cells and rat pituitary cells (as positive control) as previously described (Chomczynski and Sacchi, 1987). The total RNA from mast cells was treated with heparinase I according to Oberhauser et al. (1994) to remove native mast cell heparin, which disturbs the PCR.

The oligonucleotide primers for the substance *P* receptor PCR were purchased from MWG Biotech (Ebersberg, Germany). Primers were designed from the published cDNA sequences of rat NK_1 receptor and the rat glyceraldehyde-phosphate dehydrogenase (GAPDH). The sequences of the rat NK_1 receptor primers corresponds to bases 1371–1391 (sense) and 1735–1755 (antisense) of this receptor gene (Yokota et al., 1989). The sequence of the 5′-end digoxigenin-labeled oligonucleotide corresponds to bases 1629–1674 in the above mentioned NK_1 receptor sequence. The sequences of the rat GAPDH primers correspond to bases 478–497 (sense) and 798–817 (antisense) of this gene (Tso et al., 1985).

The Gene Amp RNA-PCR kit (Perkin-Elmer Corp., Beaconsfield, UK) was used for RT-PCR. Each sample, containing 0.5–1 μg of total cellular RNA, was reverse transcribed according to the manufacturer's protocol in the presence of oligo $d(T)_{16}$, and

Published November 1, 1998

then amplified. The amplification protocol for the rat NK_1 receptor primers was as follows: an initial 2-min cycle at 95°C, followed by 35 cycles of denaturation at 94°C for 1 min, primer annealing at 51°C for 30 s, and extension at 72°C for 45 s at the first cycle with an extension time of 2 s per cycle. After the last cycle, an extension of 7 min at 72°C was carried out. The amplification protocol for the rat GAPDH primers was: an initial 2-min cycle at 95°C, followed by 30 cycles of denaturation at 94°C for 45 s, primer annealing at 57°C for 45 s, and extension at 72°C for 45 s at the first cycle with an extension time of 1 s per cycle. After the last cycle, an extension of 7 min at 72°C was carried out. After RT-PCR, 5 μl from the 50-μl reaction mixture was electrophoresed through a 3% NuSieve agarose gel buffered with TAE (40 mM Tris-acetate, 2 mM EDTA). The gel was stained with ethidium bromide. Southern hybridization of NK_1 receptor PCR products was carried out as described previously (Winkler et al., 1995). The PCR product obtained by use of GAPDH-specific primers was cloned into the Bluescript II KS(+) plasmid and sequenced (ABI 373 system; Perkin-Elmer Cetus) with a T7 standard primer to confirm the PCR product obtained as being identical to the published cDNA sequence.

RESULTS

Translocation of SP into Mast Cells—CLSM and Electron Microscopic Autoradiography

To investigate the uptake of SP into mast cells by CLSM, fluorescein-labeled SP derivatives were synthesized. These SP analogues showed mast cell degranulating activities comparable with SP with ED_{25} (concentration required for 25% histamine release) of 15 ± 2.3, 29 ± 4.6, and 62 ± 4.1 μM for SP, all-D-SP, and FLUOS-all-D-SP, respectively. The ED_{25} for SP is higher than the reported value (Cross et al., 1995), probably due to the higher extracellular $CaCl_2$ concentration used in our experiments. A competition between Ca^{2+} and SP peptides for negatively charged binding sites on the mast cell membrane may be responsible for the observed higher value of ED_{25} for SP at the used higher Ca^{2+} concentration (Mousli et al., 1989). For translocation experiments, mast cells were pretreated with pertussis toxin to prevent degranulation artifacts.

Fig. 1 shows mast cells after incubation for 1 min in 30 μM FLUOS-all-D-SP solution and after multiple washes. An intracellular fluorescence signal is clearly visible. This signal corresponds to the intact peptide because FLUOS-all-D-SP is not degraded by mast cell proteases (D. Lorenz, unpublished results). Prolongation of the incubation time up to 32 min did not increase the fluorescence signal inside the cell, indicating that the uptake was rapid.

A more detailed insight in the kinetics of peptide uptake was obtained by experiments where the fluorescence increase was monitored in real time (Fig. 2). In these experiments, a solution containing FLUOS-all-D-SP was added via syringe and the time course of the fluorescence increase was simultaneously measured in the bath and inside the cells (Fig. 2, *B* and *C*). The intracellular fluorescence increased in parallel with growing extracellular fluorescence. The time to attain the fluorescence maximum varied only slightly, by 6 ± 4 s ($n = 3$), compared with that of extracellular fluorescence and the half-rise time, which changed by 20 ± 13 s ($n = 3$).

After establishment of a constant value of external fluorescence intensity, ~10% of the extracellular fluorescence intensity was found intracellularly. This fraction was independent of the used concentration of FLUOS-all-D-SP in the range of 0.9–8 μM, and did not change if increasing concentrations of unlabeled all-D-SP up to 200 μM were added (Fig. 3), indicating that the process was not saturable. Similar results were obtained when PtX-treated mast cells were incubated first with the unlabeled peptide, and then with the labeled peptide. Furthermore, no change in the peptide uptake was found when the cells were metabolically inhibited by antimycin or dinitrophenol (15 ± 2, 17 ± 3, and 18 ± 3% uptake with antimycin, dinitrophenol, and without metabolic inhibitors, respectively).

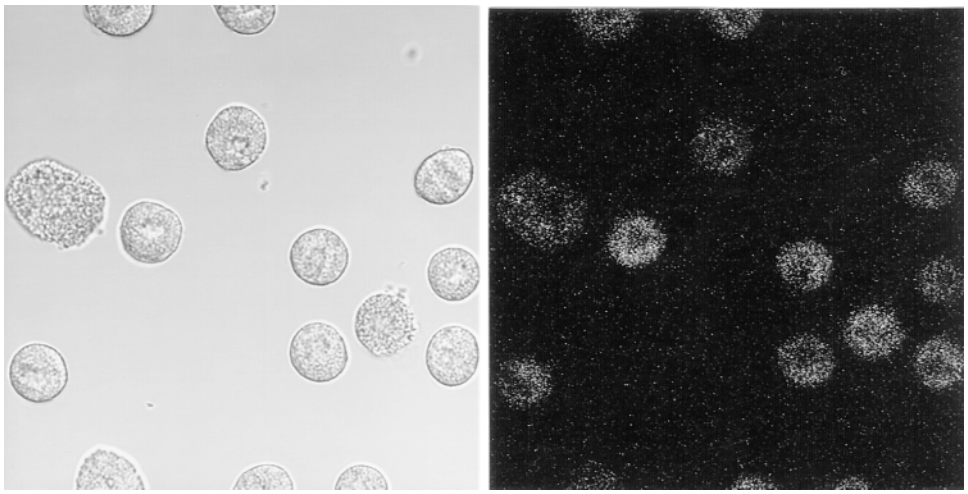

FIGURE 1. Intracellular uptake of peptide into mast cells. PtX-treated mast cells in ES were incubated for 1 min with 30 μM FLUOS-all-D-SP and subsequently washed with ES (supplemented with 6 mM $CaCl_2$ and 1 mg/ml bovine serum albumin). (*left*) Transmission image, (*right*) fluorescence image. Control cells without SP showed no fluorescence signal when monitored with the same settings of the confocal microscope as before. The scan area was adjusted to the center of mast cells.

Published November 1, 1998

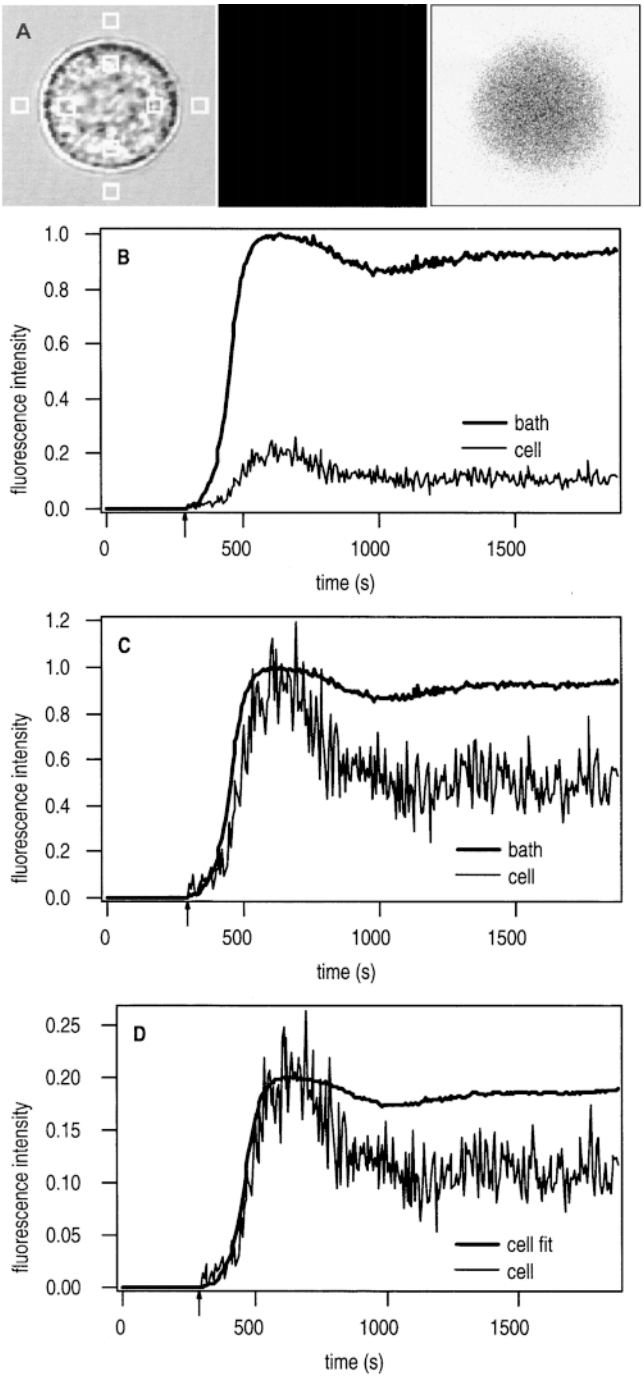

FIGURE 2. Kinetics of uptake of FLUOS-all-D-SP from extracellular medium into PtX-treated mast cells and fit of experimental data to a diffusion model. 200 μl of FLUOS-all-D-SP solution (2.5 μM) were applied via a syringe to 200 μl of ES in a dish containing mast cells adhered to the glass base of the dish. The fluorescence intensities inside and outside the cell were measured. (*A, left*) The transmission image of a mast cell before application of peptide and location of ROIs (16 × 16 pixels or 1.4 × 1.4 μm) in the scan area in the bath and inside the cell. (*middle*) The fluorescence image of the same mast cell before application of peptide. (*right*) The fluorescence image of the same cell after application of FLUOS-all-D-SP at time of maximal fluorescence intensity. (*B*) Mean fluorescence intensity inside and outside the cell from four ROIs, normalized to the highest value of extracellular fluorescence intensity; the arrow indicates the time of application of the peptide. (*C*) Mean fluorescence intensities inside and outside the cell normalized to their highest values. (*D*) Mean fluorescence intensity inside the cell as in *B* and the best fit of the data to Eq. 1 with $k_1 = 0.1\ s^{-1}$; $k_2 = 0.5\ s^{-1}$. The fitting was performed using IDL software (RSI, Boulder, CO).

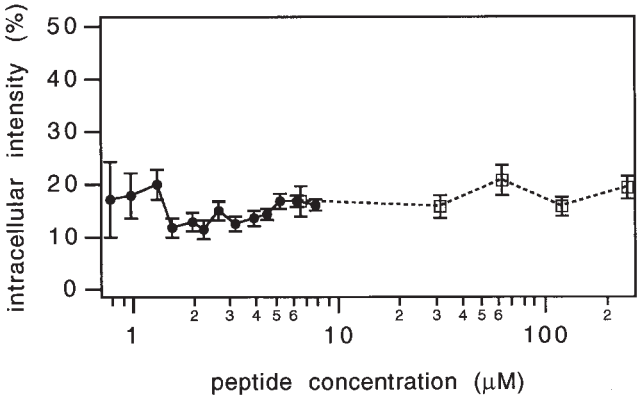

FIGURE 3. Independence of the fraction of translocated FLUOS-all-D-SP on the extracellular peptide concentration. PtX-treated mast cells were incubated for 5 min with the indicated concentrations of FLUOS-all-D-SP (●), or with 6.6 μM FLUOS-all-D-SP plus the indicated concentrations of unlabeled all-D-SP (□), and the fluorescence intensity inside and outside the cell was measured. The fraction of translocated FLUOS-all-D-SP is shown as intracellular fluorescence intensity (after background correction) normalized to the extracellular fluorescence intensity.

Eq. 1 describes the expected time course of the intracellular fluorescence intensity $I_{cell}(t)$, assuming (*a*) a simple diffusion of the peptide through the plasma membrane into the cell according to the first Fick's law, and (*b*) a direct proportional relation between fluorescence intensity and peptide concentration considering the peptide concentration as homogeneous within the cell.

$$I_{cell}(t) = k_1 \int_{t_0}^{t} I(z)\, e^{-k_2 (t-z)}\, dz, \qquad (1)$$

with $k_1 = k_2 = k$, k = rate constant of diffusion, and $I(z)$ is the measured extracellular fluorescence intensity.

No value for k was found that could give an adequate description of the experimentally observed time course $I_{cell}(t)$. A better fit of the experimental data to Eq. 1 was obtained when different values of k_1 and k_2 ($k_1 = 0.1\ s^{-1}$; $k_2 = 0.5\ s^{-1}$) were used (Fig. 2 *D*). Nevertheless, the values of the plateau of $I_{cell}(t)$ were found to be lower than the values predicted by Eq. 1 for all combinations of k_1 and k_2. This fact points to the involvement of a second process in the peptide translocation at later times, for instance a transport into a second pool inside the cell, such as a transport from the cytoplasm into the granules or other intracellular compartments. This case should be described by Eq. 2:

Published November 1, 1998

$$C_{\text{cell}}(t) = k_1 \int_{t_0}^{t} [C(z) - C_{\text{comp}}(z)]\, e^{-k_2(t-z)}\, dz, \qquad (2)$$

where $C_{\text{cell}}(z)$ is the peptide concentration in the cytoplasm, $C_{\text{comp}}(z)$ is the peptide concentration inside the second compartment, and $C(z)$ is the peptide concentration of the extracellular medium.

$C_{\text{cell}}(t)$ and also C_{comp} were not available directly from our measurements because the measured intracellular fluorescence intensity represents an average intensity over different compartments inside the cell. For this reason, only a qualitative description is performed. The lower values of the plateau of $I_{\text{cell}}(t)$ compared with the values predicted by Eq. 1 with the mentioned different k values can be explained if a decreased fluorescence intensity of the peptide inside the second compartment is assumed. In fact, an internal pH of ≤6 has been reported for mast cell granules (Lagunoff and Rickard, 1983; Johnson et al., 1980) and the fluorescence intensity of FLUOS-all-D-SP decreased by a factor of 2 when the pH was lowered from 7.2 to 5.5.

To determine the location of SP inside the cell directly, ^{3}H-labeled SP as well as ^{125}I-labeled all-D-SP and electron microscopic autoradiography were used. The results of these investigations are shown in Fig. 4. From 521 intact cells, 89% showed an intracellular labeling from ^{125}I-all-D-SP radioactivity, whereas 11% were not labeled. Interestingly, silver grains resulting from incorporated peptide showed a clearly granule-related location. 71% of silver grains were located in or on granules, 4% showed cytoplasmic location, and 25% could not be classified unequivocally to either of these locations. The plasma membrane and nucleus, however, were not labeled. Almost all sections containing a more extended part of cytoplasm free from granules (see Fig. 4 *A*) showed no labeling in this cytosolic region. Some isolated silver grains with irregular location (cytosolic space, nucleus, intercellular area) as in Fig. 4 *B* have to be considered as normal background of the photographic emulsion. These results suggest a location of incorporated peptide preferentially inside or on granules. In favor of this suggestion is also the observation that extracellular granules normally present in all preparations in clusters showed similar labeling pattern and intensity as granules inside the cells. Differences between cells incubated with ^{3}H-SP or ^{125}I-all-D-SP were limited to the number of silver grains exclusively localized in association with granules in each case. The lower frequency of radioactive signals caused by ^{3}H-SP was possibly due to a loss of peptide by degradation. An extended incubation time (10–60 min) led only to a slight

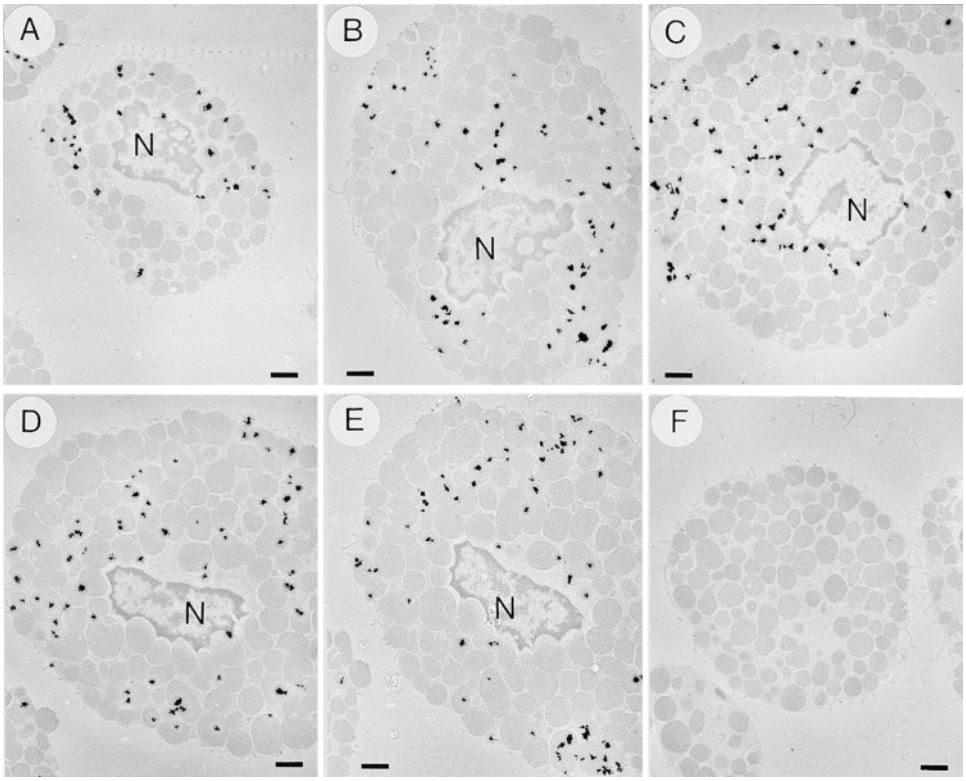

FIGURE 4. Intracellular location of translocated ^{125}I-all-D-SP in mast cells. Electron microscopic autoradiographs were obtained from PtX-treated mast cells incubated with ^{125}I-all-D-SP for 10 min and subsequently washed. *A–E* demonstrate, representatively for all investigated cells, that silver grains resulting from ^{125}I radioactivity of the incorporated peptide are clearly localized in or on granules, whereas all other cellular structures/compartments are free of such labeling. Although not every mast cell granule shows silver grains, it can be assumed that most or all of those within a cell had been in contact with substance *P*. This apparent discrepancy could be explained by the thickness of the sections (only 50 nm), autoradiographic geometrical factors, and the exposure time. An example of the possible variation regarding radioactive signals from ^{125}I-all-D-SP in/on the same granules sectioned at different levels is given by comparing *D* and *E*. *F* represents a cell from autoradiographic control specimens with unlabeled all-D-SP. Mast cells are imaged without heavy metal staining (to prevent possible artifacts in the autoradiographs) using an integrated electron energy spectrometer of the ZEISS-transmission electron microscope EM 902 A (Carl Zeiss Jena GmbH). N, nucleus. Bars = 1 μm.

Published November 1, 1998

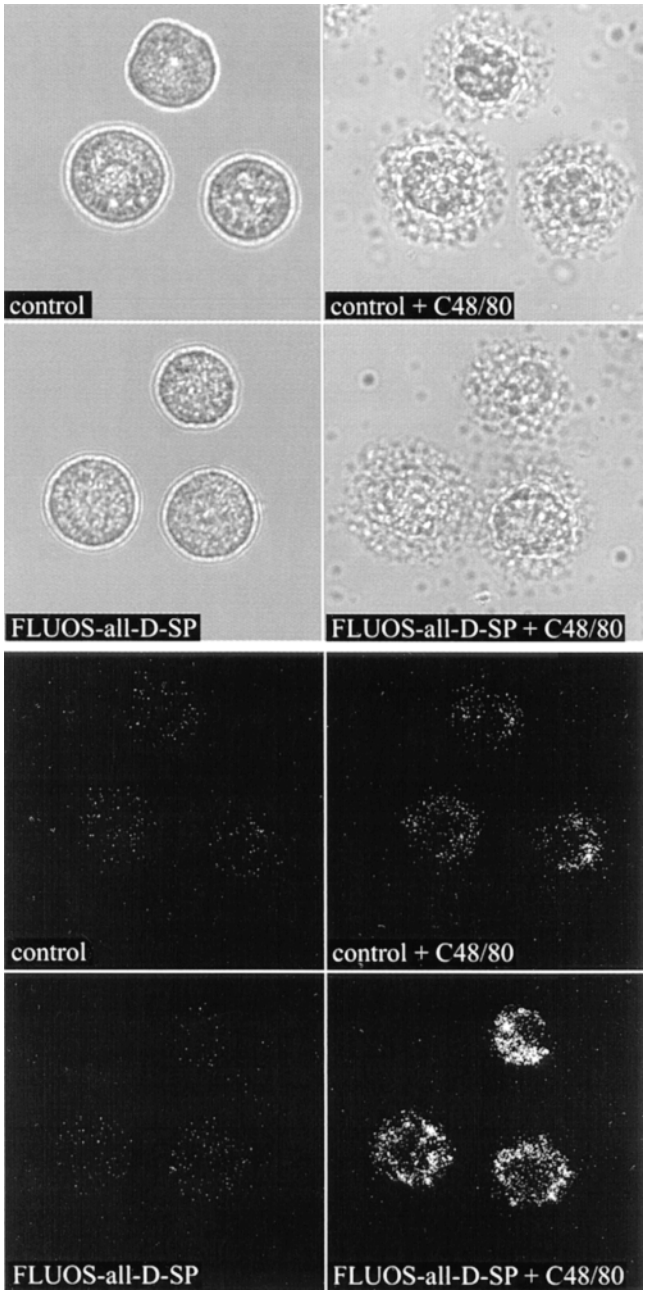

FIGURE 5. Release of FLUOS-all-D-SP translocated into mast cells stimulated with compound 48/80. Mast cells were treated with a nondegranulating dose (1 μM) of FLUOS-all-D-SP for 1 min and washed by centrifugation. Subsequently, the cells were stimulated with 24 μg/ml compound 48/80 and fluorescence was monitored 15 s after beginning of degranulation. All images were obtained with the same microscope settings. (*top*) Transmission images, (*bottom*) fluorescence images. After stimulation of degranulation with compound 48/80, the fluorescence of the three cells pretreated with SP, shown, increased by 283% (*FLUOS-all-D-SP + C48/80*). The average fluorescence increase was 109 ± 24%, n = 22, SEM. This increase is most probably due to unquenching of accumulated FLUOS-all-D-SP in just releasing granules. The small fluorescence (16 ± 17%, n = 17, SEM) observed after stimulation with compound 48/80 in controls without SP pretreatment was attributed to autofluorescence. The fluorescence in control cells pretreated with FLUOS-all-D-SP was small (absolute intensity: 7), obviously due to a great degree of quenching of accumulated FLUOS-all-D-SP in these cells.

increase in the degree of labeling of the granules. Also, an intracellular location of SP could be detected autoradiographically using native mast cells (cryostat-sectioned) at the light microscopic level (results not shown).

Preincubation of PtX-untreated mast cells with a low nondegranulating dose of FLUOS-all-D-SP, followed by washing and subsequent degranulation with compound 48/80, led to an average enhancement of fluorescence by 109 ± 24%, n = 22, SEM. For the three cells shown in Fig. 5, the fluorescence increase was 283%. These results are interpreted as follows. If translocated SP is accumulated in the secretory granules, then its fluorescence is quenched by a factor of 2 or more because of the acidic granular pH. Upon degranulation, the fusion pores open and the granular matrix will come into contact with the extracellular medium. Due to exposure of the granular matrix to this medium with higher pH, an unquenching of intragranularly located SP should occur. Therefore, in Fig. 5 the increase of fluorescence is most likely due to unquenching of FLUOS-all-D-SP-fluorescence in just releasing granules. The cells exhibited a great variability in the fluorescence increase, probably due to differences in the uptake and/or differences in the granular pH resulting in different degrees of quenching. The small increase of fluorescence in control cells without SP pretreatment (16 ± 17%, n = 17, SEM) might be the result of autofluorescence. The control cells with peptide pretreatment showed a similar low fluorescence signal as the controls without peptide pretreatment at the microscope settings used. The low fluorescence of the pretreated cells is obviously due to a large degree of quenching of accumulated FLUOS-all-D-SP in these PtX-untreated cells. The results shown demonstrate directly that extracellularly applied SP translocates across the plasma membrane and accumulates in the secretory granules.

Intracellular Action of SP–Patch-Clamp Measurements

To test if intracellularly applied peptide stimulates mast cell degranulation, the patch-clamp technique in the whole-cell mode was used. SP was directly applied via the patch pipette and the time course of degranulation was measured by determining the electrical capacitance C_m of the cell membrane. For comparison, the time course of capacitance increase was also determined for the nonhydrolyzable GTP analogue GTPγS, known to stimulate mast cell degranulation when intracellularly applied (Fernandez et al., 1984).

A typical time course for the degranulation of a mast cell dialyzed with 25 μM SP in low Ca^{2+} buffering conditions is shown in Fig. 6. The process was character-

Published November 1, 1998

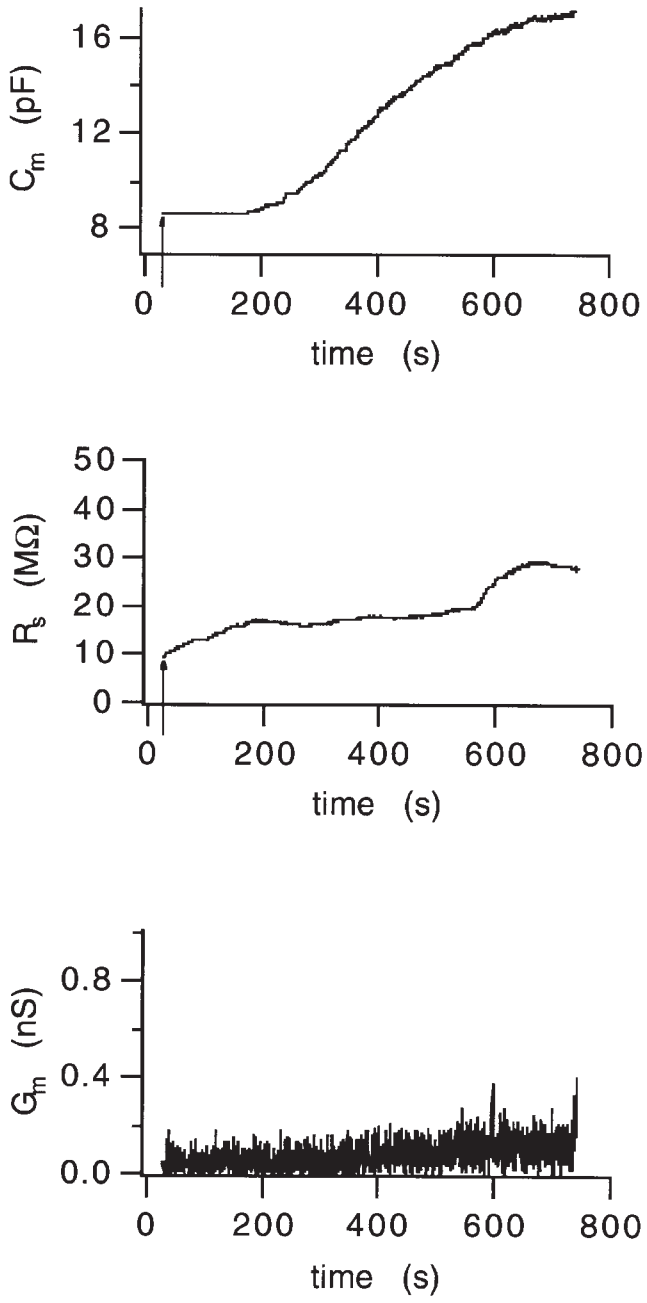

FIGURE 6. Mast cell degranulation induced by intracellular application of SP. The time course of mast cell degranulation after dialysis of SP through the patch pipette was measured as increase of membrane capacitance (*top*). Series resistance *(middle)*, and membrane conductance *(bottom)*. Pipette solution: IS 1 with 200 μM EGTA and 25 μM SP. Arrow indicates time of patch rupture.

ized by a time delay before the onset of degranulation (for this cell, 250 s). The degranulation proceeded for up to 500 s and led to a pronounced increase of C_m. Of 47 cells internally perfused with IS 1 containing SP at different concentrations, 66% degranulated within 15–20 min. In the degranulating cells, the membrane capacitance increased by a factor of 2.1 ± 0.1, $n = 31$. A statistically significant dependence of the overall capacitance increase on peptide concentration was not detected. It is noteworthy that intracellular concentrations of SP as low as 5 ($n = 11$) and 1 ($n = 3$) μM stimulated mast cell degranulation, whereas, at these concentrations, no degranulation was found in mast cell suspensions when the peptide was applied extracellularly. This suggests that SP acts at an intracellular site.

Only 18% of control cells dialyzed internally with IS 1 in the absence of SP (4 of 22) showed spontaneous degranulation after 20 min, and in these four cells degranulation started after a long delay (10–15 min) and was slow.

When GTPγS was applied at similar concentrations, degranulation occurred in 41 of 45 cells and the total capacitance increase was 2.7 ± 0.1-fold.

GDPβS applied together with SP through the patch-pipette (1 mM GDPβS, 5 μM SP) inhibited exocytosis in four of five cells tested. Likewise, pretreatment of mast cells with PtX for 7–9 h led to inhibition of degranulation induced by 25 μM SP ($n = 4$), whereas all control cells incubated for the same time without PtX degranulated ($n = 3$). However, treatment with PtX for shorter times (4 h) failed to give an adequate effect. These results strongly suggest that intracellular application of SP stimulates exocytosis via activation of GTP-binding proteins. This is further supported by several similarities between stimulation with GTPγS and SP. As previously reported (Fernandez et al., 1987), the time

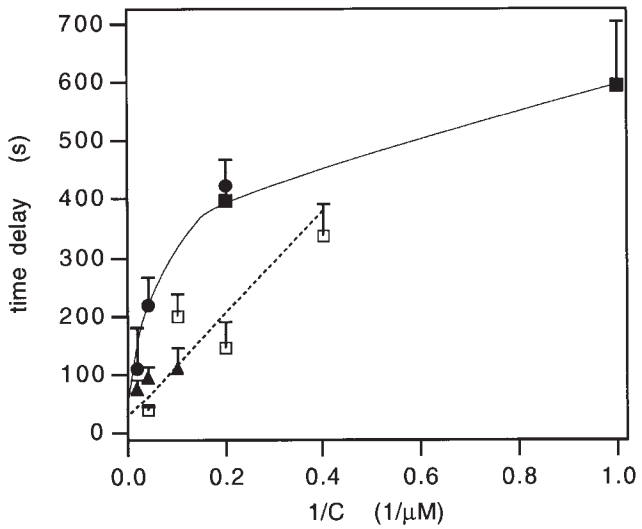

FIGURE 7. Time delay of mast cell degranulation in response to intracellular application of SP (*solid line*) or GTPγS (*dotted line*) through the patch pipette. Dependence on inverse concentration (1/C) and effect of $MgCl_2$ on the delay for SP. (● and ■) SP with 7 mM $MgCl_2$ (IS 1); (▲) SP with 1 mM $MgCl_2$ (IS 2); (□) GTPγS with 7 mM $MgCl_2$ (IS 1). In all cases, the pipette solution contained 200 μM EGTA without Ca^{2+}, except ■, where the free Ca^{2+} concentration was 240 nM. (*dotted line*) Linear regression line for GTPγS; (*solid line*) free hand line drawn for SP with 7 mM $MgCl_2$.

Published November 1, 1998

delay depends linearly on the reciprocal GTPγS concentration (Fig. 7). Similarly, in SP-stimulated cells, the time delay decreased with increasing peptide concentrations of SP (Fig. 7). In IS 1 containing 7 mM $MgCl_2$, the delay was longer than that observed for the G-protein activator GTPγS when applied at the same concentrations (Fig. 7). The shortest time delay obtained by extrapolating the curves in Fig. 7 to high concentrations was about 20 s for GTPγS, in agreement with previous data (Fernandez et al., 1987), and 50 s for SP. The degranulation rate for SP was found to be 0.045 ± 0.008 pF/s (1–25 μM, n = 27) and 0.08 ± 0.01 pF/s (50 μM, n = 4); for GTPγS, the degranulation rate increased from 0.05 ± 0.005 pF/s at 2.5–5 μM (n = 25) to 0.15 ± 0.03 pF/s at 10–25 μM (n = 16).

Reduction of the $MgCl_2$ concentration in the intracellular solution from 7 to 1 mM (IS 2) led to a decrease in the time delay of SP-induced exocytosis (Fig. 7). The degranulation rate increased approximately twofold compared with that in IS 1. Under these conditions, 15 of 25 cells degranulated with 10–50 μM SP and none of the control cells dialyzed with IS 2 showed

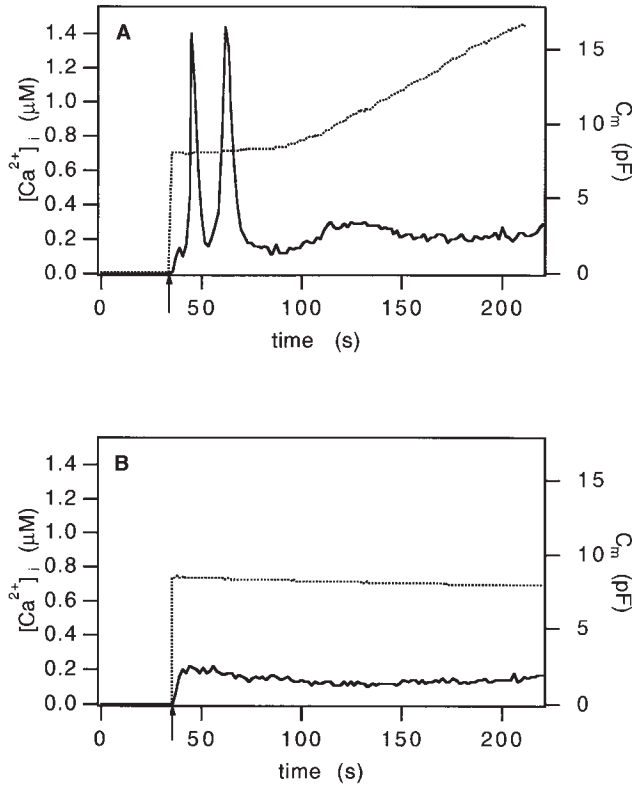

FIGURE 8. Intracellular calcium transients in mast cells induced by intracellular application of SP. Simultaneously measured time courses of intracellular free Ca^{2+} concentration (*solid line*) and capacitance (*dotted line*) with (*A*) and without (*B*) intracellular application of SP through the patch pipette. Pipette solution: IS 2 with or without 10 μM SP, and 100 μM FURA-2 and 100 μM EGTA. The arrow indicates the time of patch rupture.

any sign of degranulation (n = 7). Omission of ATP in the pipette abolished the SP-induced degranulation (n = 4).

To estimate the time required for SP to diffuse into the cell, fluorescence measurements were done using FLUOS-all-D-SP. For R_s in the range 9–20 MΩ, a diffusion half time constant τ_D = 18.2 ± 4 s (n = 4) was obtained. Thus, diffusional exchange between pipette and the cell interior is rapid.

As for GTPγS (Neher, 1988), the intracellular application of SP caused transient rises followed by an elevated level of $[Ca^{2+}]_i$ (Fig. 8). The onset of capacitance increase occurred subsequent to the transient increase of $[Ca^{2+}]_i$. Controls without SP showed a resting level of 140–200 nM of free Ca^{2+}.

Intracellular application of all-D-SP (25–200 μM) also induced mast cell degranulation with a delay of 440 ± 100 s, n = 27 (IS 1 with 400 μM EGTA). The time delay of the intracellular mast cell stimulation depended on the Ca^{2+}-buffering conditions used, indicating a dependence on intracellular free Ca^{2+} concentration. In weakly buffered conditions (200 μM EGTA), when the intracellular Ca^{2+} concentration was not under the control of the pipette (Neher, 1988; Lindau and Gomperts, 1991), a delay of 168 ± 77 s (n = 7) was observed for 100 μM all-D-SP, whereas, in stronger buffering conditions (1,200 μM EGTA), no degranulation occurred.

In addition to the SP derivatives mentioned above, we tested SP(1-4)dodecylamide, which caused mast cell degranulation with a 10-fold lower ED_{25} compared with SP when applied extracellularly (Repke et al., 1987). At a concentration of 1 μM, this analogue showed an intracellular stimulation of mast cell degranulation with a time delay of 303 ± 85 s (n = 7) (IS 1 with 200 μM EGTA).

RT-PCR

The PCR product of the NK_1 receptor in the pituitary samples, used as positive control for NK_1 receptor mRNA, had the predicted size of 380 bp (Fig. 9 *A*). Furthermore, the specificity was confirmed by hybridization with an NK_1 receptor-specific DIG-labeled oligonucleotide. RNA isolated from mast cells did not give an adequate signal in the RT-PCR reaction (Fig. 9 *A*).

The quality of the RNA preparation of mast cells was checked in another RT-PCR with primers specific for GAPDH. The PCR products showed an adequate signal in both mast and pituitary cells (Fig. 9 *B*).

DISCUSSION

The mechanism of peptide-induced mast cell activation has been unclear, although a variety of studies concerning this problem have been undertaken. It had been

Published November 1, 1998

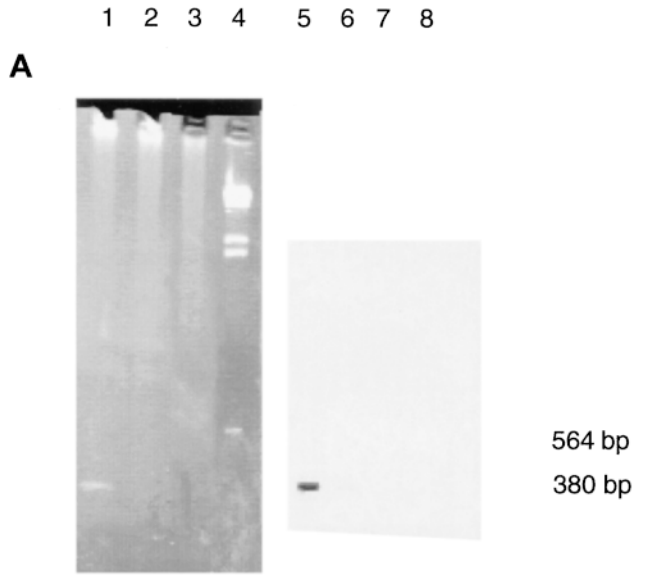

FIGURE 9. Analysis of RT-PCR products obtained by the use of SP-receptor–specific primers (*A*), and by use of GAPDH-specific primers (*B*). (*A*) Lanes *1* and *5*, positive control (rat pituitary, 1 μg total RNA); lanes *2* and *6*, mast cells (0.5 μg total RNA); lanes *3* and *7*, mast cells (1 μg total RNA), lanes *4* and *8*, DNA marker, λ/Hind III. (*B*) Lane *1*, DNA marker, λ/Hind III; lane *2*, rat pituitary (0.5 μg total RNA); lane *3* mast cells (0.5 μg total RNA); lane *4* negative control (RNA without reverse transcription). Lanes *1–4*, 3% agarose gel, ethidium bromide stained; lanes *5–8*, Southern blot hybridized with SP receptor digoxigenin-labeled oligonucleotide.

suggested (Mousli et al., 1990*b*) that the peptides interact directly with heterotrimeric G proteins, thereby mimicking the receptor. Such a mechanism would require a deep insertion of peptides into the membrane and/or their translocation into the cytoplasm of mast cells. According to this model, intracellular application of SP should induce mast cell exocytosis. The aim of the present investigation was to answer the questions: (*a*) Do SP-specific receptors exist in the plasma membrane of rat peritoneal mast cells? (*b*) Can extracellularly applied SP be translocated into mast cells? and (*c*) Is intracellularly applied SP able to induce mast cell degranulation?

Using RT-PCR (Fig. 9, *A* and *B*), no SP receptor-specific mRNA was detected in mast cells, whereas mRNA for GAPDH (a "housekeeping" gene expressed in all cells) used as quality control for the DNA preparation was demonstrable in these cells; moreover, in rat pituitary cells, mRNAs for both SP receptor and GAPDH were found. These results support the view of a SP-receptor–independent action of SP on mast cells.

For the investigation of the uptake of SP into mast cells by CLSM, the fluorescence-labeled SP derivatives FLUOS-SP and FLUOS-all-D-SP were synthesized. These analogues showed pronounced histamine releasing activity, but the dose–response curve of the all-D analogues was shifted to higher concentrations compared with SP. The all-D-SP was used because of its high enzymatic stability. Therefore, an uptake of peptide degradation products into mast cells during translocation experiments could be excluded.

The pertussis toxin treatment, performed to prevent artifacts associated with degranulation, did not disturb the integrity of the plasma membrane as revealed from electron microscopic observations and from trypan blue staining. In addition, the non–membrane-penetrating dyes carboxyfluorescein and BSA-rhodamine were not translocated into PtX-treated mast cells (Wiesner et al., manuscript in preparation).

The results obtained by CLSM directly show translocation of SP peptides into PtX-treated cells (Figs. 1–3). The kinetic experiments (Fig. 2, *B* and *C*) indicated that the translocation process was rapid, occurring within a few seconds. After the maximum was reached, the fluorescence intensity decayed to a greater extent inside the cell than in the outside medium (Fig. 2 *C*), indicating that an additional decay process is superimposed on the uptake process. Photobleaching of FLUOS peptides by the laser was precluded by control experiments and the use of all-D analogues of SP eliminated any possible loss of peptide due to peptide degradation. The results of modeling the time course of uptake of SP using diffusion models led to the proposal that a second translocation process should take place such as an uptake into mast cell granules, where the fluorescence of the peptide is quenched. The results of CLSM experiments are directly supported by the electron microscopic autoradiography (Fig. 4) and by experiments shown in Fig. 5. Electron microscopic autoradiography with ^{125}I-all-D SP and ^{3}H-SP demonstrated a location of SP preferentially on or inside the granules (Fig. 4). However, SP was not found in the nucleus, the cytoplasm, or on the plasma membrane. The latter finding is not surprising because SP bound to the plasma membrane was removed by washing. Furthermore, a radioactive staining on the cytosolic side of the membrane due to the proposed interaction of the "receptor-mimicking" SP with membrane-bound $G_{i/o}$ proteins is not likely because such interactions are blocked by PtX treatment. The autoradiographic resolution does not

Published November 1, 1998

allow a conclusion as to whether SP is located on the granule membrane and/or within the granules. However, SP is most likely located at least partly inside the granules, as indicated by the fact that an increase of fluorescence intensity occurred when mast cells, preloaded with a nondegranulating dose of the fluorescent peptide, were stimulated by compound 48/80. The degranulation results in an exposure of the granular matrix to the extracellular medium with higher pH and, therefore, in a rise of fluorescence of intragranularly localized peptide (Fig. 5).

Secretory granules of mast cells contain a heparin proteoglycan matrix (Sayama et al., 1987), which is negatively charged at the granular acidic pH. Recently, it was demonstrated (Parpura and Fernandez, 1996) that this matrix behaves as an ion-exchange resin. On the other hand, strong binding of cationic peptides to negatively charged ion exchangers possessing hydrophobic groups (e.g., Dowex) has been shown (Berger et al., 1982). This may explain binding of positively charged SP to the granule matrix. The independence of peptide uptake on concentration and the finding that the uptake is not saturable in the concentration range used (Fig. 3) is in agreement with the accumulation and binding of SP inside the granules. However, binding of SP to other proteins on the granular membrane or inside the granule cannot be excluded and remains to be elucidated.

The mechanism by which the transport of cationic peptides into mast cells takes place is unknown. The short time of translocation suggests mechanisms independent of classical endocytosis, which typically has shown half-lives >10 min. Nonspecific diffusion of SP peptides due to membrane damage could be excluded since cells showed trypan blue exclusion for at least 5 min after the translocation experiments. The absence of a saturable uptake (Fig. 3) and the fact that metabolically inhibited cells have the same uptake suggest that active transporters are not involved in the translocation process. This is in agreement with recently reported studies of the energy-independent translocation of peptides derived from the third helix of Antennapedia homeodomain into neuronal cells (Derossi et al., 1994). Cellular uptake of peptides derived from HIV-1 Tat protein (Vivès et al., 1997) and from the hydrophobic region of various protein signal sequences (Lin et al., 1995; Lui et al., 1996) and of model peptides (Oehlke et al., 1996, 1997) was previously demonstrated. Interestingly, large transmembrane movements of segments of the protein toxin colicin and inserted foreign epitopes across planar lipid bilayer membranes associated with channel opening and closing were recently observed (Qiu et al., 1996; Jakes et al., 1998). The authors suggest that a small part of colicin itself acts as a nonspecific translocator. Furthermore, it was found that peptides such as mitochondrial presequences (Maduke and Roise, 1993) or magainin 2 and mastoparan (Matzusaki et al., 1995, 1996) are imported into liposomes. These peptides are relatively large and it was suggested (Matzusaki et al., 1995) that they can adopt an amphipathic helical, membrane-spanning conformation, building a short-lived pore (~40 μs lifetime). The pore formation is thought to be coupled with peptide translocation. However, SP is too short to adopt such a membrane-spanning conformation; thus, another mechanism must be responsible for SP peptide translocation.

One mechanism of uptake of SP without entering the cytoplasm at all might be diffusion of the peptide into the secretory granules through flickering fusion pores (Alvarez de Toledo et al., 1993). This is not likely because PtX inhibited degranulation when SP uptake was measured. In addition, we also observed an uptake into aortic endothelial and HEK293 cells (Oehlke et al., 1997; D. Lorenz and B. Wiesner, unpublished data).

The patch-clamp measurements indicated that intracellularly applied peptide activates mast cell degranulation (Figs. 6 and 8). However, SP showed a longer time delay compared with the G-protein activator GTPγS (Fig. 7), and the degranulation amplitude was somewhat reduced. The diffusion of the peptide from the patch pipette into the cell seems not to be responsible for the observed time delay because diffusional time measurements demonstrated a fast diffusional exchange of peptide between pipette and the cell interior.

Nonspecific membrane-perturbing effects of the peptide leading to degranulation are unlikely, because in the absence of ATP the intracellular stimulation by the peptide was abolished. The fact that GDPβS and pertussis toxin treatment inhibited the SP-induced intracellular activation points to the involvement of heterotrimeric G proteins. The observation that reduction of the free Mg^{2+} concentration in the patch pipette from 7 to 1 mM decreased the time delay (Fig. 7) further supports G protein involvement. It has been shown that the activation of heterotrimeric $G_{i/o}$ proteins by cationic peptides is reduced at high millimolar Mg^{2+} concentrations (Higashijima et al., 1990). However, other Mg^{2+}-dependent cellular events might be involved. SP induced fast transient rises in $[Ca^{2+}]_i$ (Fig. 8), presumably as a result of Ca^{2+} release from internal stores due to G protein–mediated activation of PLC by intracellularly applied SP. The elevated level of $[Ca^{2+}]_i$ following the transients was similar to those observed when SP or compound 48/80 was applied extracellularly to mast cells (Penner et al., 1988; Matthews et al., 1989) and has been shown to be the result of activation of Ca^{2+}-release–activated Ca^{2+} channels and of nonspecific cation channels (Hoth and Penner, 1992; Fasalato et al., 1993; Kuno et al., 1989).

The patch-clamp results show that intracellularly applied SP stimulates mast cell degranulation, suggesting

a direct activation of heterotrimeric PtX-sensitive G proteins linked to PLC activation and release of Ca^{2+} from internal stores. Whether the recently found G_{i3}, thought to act downstream of PLC to trigger exocytosis (Aridor et al., 1990, 1993), and/or other G proteins are activated directly by intracellularly applied SP cannot be ascertained from the presented data. The inhibition of exocytosis found when $[Ca^{2+}]_i$ was clamped to low values by EGTA suggests that a certain level of free Ca^{2+} is necessary for the SP-induced exocytosis. Obviously, as reported previously (Lillie and Gomperts, 1993), Ca^{2+} modulates degranulation by enhancing the sensitivity for GTP of the G protein downstream of PLC. Also, the possible additional involvement of other proteins cannot be excluded. Activation of the nucleoside diphosphate kinase in HeLa cells by the cationic peptide mastoparan has been reported (Klinker et al., 1994), resulting in transphosphorylation of GDP to GTP in the presence of ATP, and thereby maintaining a pool of available GTP. Likewise, an inhibition of GTPase-activating proteins cannot be ruled out.

That a cationic peptide can stimulate mast cell degranulation intracellularly was observed also by Oberhauser et al. (1992). Synthetic peptides, corresponding to the putative effector domain of the small G protein rab 3, were reported to stimulate exocytosis in patch-clamped mast cells (Oberhauser et al., 1992). It was suggested that rab 3 peptides act directly on the effector protein, which is part of the protein macrocomplex of the exocytotic fusion pore. On the other hand, rab 3-like peptides have been shown to stimulate exocytosis via a PtX-sensitive G protein when applied extracellularly (Law et al., 1993). They were able to induce Ca^{2+} transients and did not stimulate exocytosis when cells were treated with PtX. Interestingly, these peptides show similarities in their structure with mastoparan, known to stimulate purified G_i proteins and mast cell exocytosis. Induction of exocytosis by mastoparan has also been demonstrated in permeabilized AtT 20 cells (McFerran and Guild, 1995). In permeabilized chromaffin cells, mastoparan showed inhibitory as well as stimulatory effects on exocytosis, depending on the absence or presence of MgATP and Mg^{2+} (Vitale et al., 1996).

In summary, our study demonstrates that SP is translocated into mast cells in an energy- and SP-receptor–independent fashion. Inside the cell, the peptide was found to be exclusively in or on the mast cell granules. Intracellularly applied peptide induced exocytosis, which was blocked by GDPβS and PtX treatment, suggesting the involvement of heterotrimeric G proteins. Simultaneous measurements of degranulation and of the intracellular free Ca^{2+} concentration demonstrated directly that the heterotrimeric G protein linked to PLC activation was stimulated by intracellularly applied SP. However, the involvement of other proteins cannot be excluded and remains to be elucidated. Thus, SP-induced activation of isolated mast cells seems to be a receptor-independent process, initiated by binding of SP to negatively charged binding sites on the plasma membrane and followed by a translocation of peptide into the mast cell, where it stimulates G proteins directly.

The authors thank I. Gogalla and B. Oczko for their excellent technical assistance, and Dr. K. Fechner and J. Dicksen for the critical reading of the manuscript.

Original version received 27 May 1998 and accepted version received 21 August 1998.

REFERENCES

Alvarez de Toledo, G., G. Fernández-Chacón, and J.M. Fernández. 1993. Release of secretory products during transient vesicle fusion. *Nature.* 363:554–558.

Aridor, M., L.M. Traub, and R. Sagi-Eisenberg. 1990. Exocytosis in mast cells by basic secretagogues: evidence for direct activation of GTP-binding proteins. *J. Cell Biol.* 111:909–917.

Aridor, M., G. Rajmilevich, M.A. Beaven, and R. Sagi-Eisenberg. 1993. Activation of exocytosis by the heterotrimeric G-protein G_{i3}. *Science.* 262:1569–1572.

Berger, H., H. Schäfer, E. Klauschenz, E. Albrecht, and B. Mehlis. 1982. Rapid assay for in vitro degradation of luteinizing hormone releasing hormone. *Anal. Biochem.* 127:418–425.

Bueb, J.-L., M. Mousli, C. Bronner, B. Rouot, and Y. Landry. 1990. Activation of Gi-like proteins, a receptor-independent effect of kinins in mast cells. *Mol. Pharmacol.* 38:816–822.

Cockcroft, S., T.W. Howell, and B.D. Gomperts. 1987. Two G-proteins act in series to control stimulus-secretion conpling in mast cells: use of neomycin to distinguish between G-proteins controlling polyphosphoinositide phosphodiesterase and exocytosis. *J. Cell Biol.* 105:2745–2750.

Chomczynski, P., and N. Sacchi. 1987. Single step method of RNA isolation by acid guanidinium thiocyanate-phenol-chloroform extraction. *Anal. Biochem.* 162:156–162.

Cross, M.L.J., M. Ennis, E. Krause, M. Dathe, D. Lorenz, G. Krause, M. Beyermann, and M. Bienert. 1995. Influence of α-helicity, amphipathicity and D-amino acid incorporation on the peptide-induced mast cell activation. *Eur. J. Pharmacol.* 291:291–300.

Cross, M.L.J., A.G. Beck-Sickinger, M. Beyermann, E. Krause, M. Bienert, and M. Ennis. 1993. Neuropeptide Y-induced mast cell activation. *Biochem. Soc. Trans.* 22:7S.

Derossi, D., A.H. Joliot, G. Chassaing, and A. Prochiantz. 1994. The third helix of the antennapedia homeodomain translocates through biological membranes. *J. Biol. Chem.* 269:10444–10450.

Emadi-Khiav, B., M. Mousli, C. Bronner, and Y. Landry. 1995. Human and rat cutaneous mast cells: involvement of a G-protein in the response to peptidergic stimuli. *Eur. J. Pharmacol.* 272:97–102.

Fasalato, C., M. Hoth, G. Matthews, and R. Penner. 1993. Ca^{2+} and Mn^{2+} influx through receptor-mediated activation of nonspecific cation channels in mast cells. *Proc. Natl. Acad. Sci. USA*. 90:3068–3072.

Fernandez, J.M., E. Neher, and B.D. Gomperts. 1984. Capacitance measurements reveal stepwise fusion events in degranulating mast cells. *Nature* . 312:453–455.

Fernandez, J.M., M. Lindau, and F. Eckstein. 1987. Intracellular stimulation of mast cells with guanine nucleotides mimic antigenic stimulation. *FEBS Lett.* 216:89–93.

Fischer, T., C. Bronner, Y. Landry, and M. Mousli. 1993. The mechanism of inhibition of alkylamines on the mast cell peptidergic pathway. *Biochim. Biophys. Acta* . 1176:305–312.

Gundemar, L., and R. Håkanson. 1991. Neuropeptide Y, peptide YY and C-terminal fragments release histamine from rat peritoneal mast cells. *Br. J. Pharmacol.* 104:776.

Higashijima, T., J. Burnier, and E.M. Ross. 1990. Regulation of Gi and Go by mastoparan, related amphiphilic peptides and hydrophobic amines. *J. Biol. Chem.* 265:14176–14186.

Hoth, M., and R. Penner. 1992. Depletion of intracellular calcium stores activates a calcium current in mast cells. *Nature.* 335:353–355.

Jakes, K.S., P.K. Kienker, S.L. Slatin, and A. Finkelstein. 1998. Translocation of inserted foreign epitopes by a channel-forming protein. *Proc. Natl. Acad. Sci. USA.* 95:4321–4326.

Johnson, R.G., S.E. Carty, B.J. Fingerhood, and A. Scarpa. 1980. The internal pH of mast cell granules. *FEBS Lett.* 120:75–79.

Klinker, J.F., A. Hagelüken, L. Grünbaum, I. Heilmann, B. Nürnberg, R. Harhammer, S. Offermanns, I. Schwaner, J. Ervens, K. Wenzel-Seifert, et al. 1994. Mastoparan may activate GTP hydrolysis by G_i-proteins in HL-60 membranes indirectly through interaction with nucleoside diphosphate kinase. *Biochem. J.* 304:377–383.

Kuno, M., T. Okada, and T. Shibata. 1989. A patch-clamp study: secretagogue-induced currents in rat peritoneal mast cells. *Am. J. Physiol.* 256:C560–C568.

Lagunoff, D., and A. Rickard. 1983. Evidence for control of the mast cell granule protease in situ by low pH. *Exp. Cell Res.* 144: 353–360.

Landry, Y., C. Bronner, M. Mousli, T. Fischer, and A. Vallé. 1992. The activation of mast cells: molecular targets and transducing processes for antigenic and non-antigenic stimuli. *Bull. Inst. Pasteur.* 90:83–98.

Law, G.J., A.J. Northrop, and W.T. Mason. 1993. Rab3-peptide stimulates exocytosis from cells via a pertussis toxin-sensitive mechanism. *FEBS Lett.* 333:56–60.

Lillie, T.H.W., and B.D. Gomperts. 1992. Guanine nucleotide is essential and Ca^{2+} is a modulator in the exocytotic reaction of permeabilized rat mast cells. *Biochem. J.* 288:181–187.

Lillie, T.H.W., and B.D. Gomperts. 1993. GTPase as regulators of regulated secretion. *In* GTPases in Biology I. B.F. Dickey and L. Birnbaumer, editors. Springer-Verlag, Berlin, Germany. 661–678.

Lin, Y.-Z., S.Y. Yao, R.A. Veach, T.R. Torgerson, and J. Hawiger. 1995. Inhibition of nuclear translocation of transcription factor NF-κB by a synthetic peptide containing a cell membrane-permeable motif and nuclear localization sequence. *J. Biol. Chem.* 270: 14255–14258.

Lindau, M., and O. Nüße. 1987. Pertussis toxin does not affect the time course of exocytosis in mast cells stimulated by intracellular application of GTP-γ-S. *FEBS Lett.* 222:317–321.

Lindau, M., and E. Neher. 1988. Patch-clamp techniques for time-resolved capacitance measurements in single cells. *Pflügers Arch.* 411:137–146.

Lindau, M., and B.D. Gomperts. 1991. Techniques and concepts in exocytosis: focus on mast cells. *Biochim. Biophys. Acta.* 1071:429–471.

Lui, X.-Y., S. Timmons, Y.-Z. Lin, and J. Harwiger. 1996. Identification of a functionally important sequence in the cytoplasmic tail of integrin β_3 by using cell permeable peptide analogs. *Proc. Natl. Acad. Sci. USA.* 93:11819–11824.

Maduke, M., and D. Roise. 1993. Import of a mitichondrial presequence into protein-free phospholipid vesicles. *Science.* 260:364–367.

Marshall, J.S., and S. Waserman. 1995. Mast cells and the nerves—potential interactions in the context of chronic disease. *Clin. Exp. Allergy.* 25:102–110.

Matthews, G., E. Neher, and R. Penner. 1989. Second messenger-activated calcium influx in rat peritoneal mast cells. *J. Physiol. (Camb.).* 418:105–130.

Matzusaki, K., O. Murase, and K. Miyajima. 1995. Kinetics of pore formation by an antimicrobial peptide, magainin 2, in phospholipid bilayers. *Biochemistry.* 34:12553–12559.

Matzusaki, K., S. Yoneyama, O. Murase, N. Fujii, and K. Miyajima. 1996. Transbilayer transport of ions and lipids coupled with mastoparan X translocation. *Biochemistry.* 35:8450–8456.

McFerran, B.W., and S.B. Guild. 1995. Effects of mastoparan upon the late stages of the ACTH secretory pathway of AtT-20 cells. *Br. J. Pharmacol.* 115:696–702.

McKay, D.M., and J. Bienenstock. 1994. The interaction between mast cells and nerves in the gastrointestinal tract. *Immunol. Today.* 15:533–538.

Mousli, M., C. Bronner, J.-L. Bueb, E. Tschirhart, J.-P. Gies, and Y. Landry. 1989. Activation of rat peritoneal mast cells by substance *P* and mastoparan. *J. Pharmacol. Exp. Ther.* 250:329–335.

Mousli, M., C. Bronner, Y. Landry, J. Bockaert, and B. Rouot. 1990*a*. Direct activation of GTPbinding regulatory proteins (G-proteins) by substance *P* and compound 48/80. *FEBS Lett.* 259: 260–262.

Mousli, M., J.-W. Bueb, C. Bronner, B. Rouot, and Y. Landry. 1990*b*. G-protein activation: a receptor-independent mode of action for cationic amphiphilic neuropeptides and venom peptides. *Trends Pharmacol. Sci.* 11:358–362.

Mousli, M., T.E. Hugli, Y. Landry, and C. Bronner. 1994. Peptidergic pathway in human skin and rat peritoneal mast cell activation. *Immunopharmacology.* 27:1–8.

Mousli, M., A. Trifilieff, J.T. Pelton, J.-P. Gies, and Y. Landry. 1995. Structural requirements for neuropeptide Y in mast cells and G-protein activation. *Eur. J. Pharmacol.* 289:125–133.

Neher, E. 1988. The influence of intracellular calcium concentration on degranulation of dialysed mast cells from rat peritoneum. *J. Physiol. (Camb.).* 395:193–214.

Neher, E., and R.S. Zucker. 1993. Multiple calcium-dependent processes related to secretion in bovine chromaffin cells. *Neuron.* 10:21–30.

Nüße, O., and M. Lindau. 1990. GTPγS-induced calcium transients and exocytosis in human neutrophils. *Biosci. Rep.* 10:93–103.

Oberhauser, A.F., V. Balan, C.L. Fernandez-Badilla, and J.M. Fernandez. 1994. RT-PCR cloning of Rab 3 isoforms expressed in peritoneal mast cells. *FEBS Lett.* 339:171–174.

Oberhauser, A.F., J.R. Monck, W.E. Balch, and J.M. Fernandez. 1992. Exocytotic fusion is activated by Rab3a peptides. *Nature.* 360:270–273.

Oehlke, J., E. Krause, B. Wiesner, M. Beyermann, and M. Bienert. 1996. Nonendocytic, amphipathicity dependent cellular uptake of helical model peptides. *Protein Pept. Lett.* 3:393–398.

Oehlke, J., E. Krause, B. Wiesner, M. Beyermann, and M. Bienert. 1997. Extensive cellular uptake into endothelial cells of an amphipathic β-sheet forming peptide. *FEBS Lett.* 415:196–199.

O'Flynn, N.M., R.D. Helme, D.J. Watkins, and E. Burcher. 1989.

Autoradiographic localization of substance *P* binding sites in rat footpad skin. *Neurosci. Lett.* 106:43–48.

Parpura, V., and J.M. Fernandez. 1996. Atomic force microscopy study of the secretory granule lumen. *Biophys. J.* 71:2356–2366.

Paton, W.D.M. 1951. Compound 48/80: a potent histamine releaser. *Brit. J. Pharmacol.* 6:499–508.

Penner, R. 1988. Multiple signaling pathways control stimulus-secretion coupling in rat peritoneal mast cells. *Proc. Natl. Acad. Sci. USA.* 85:9856–9860.

Penner, R., G. Matthews, and E. Neher. 1988. Regulation of calcium influx by second messengers in rat mast cells. *Nature.* 334: 499–504.

Purcell, W.M., K.M. Doyle, C. Westgate, and C.K. Atterwill. 1996. Characterisation of a functional polyamine site on rat mast cells: association with a NMDA receptor macrocomplex. *J. Neuroimmunol.* 65:49–53.

Purcell, W.M., and C.K. Atterwill. 1995. Mast cells in neuroimmune function: neurotoxicological and neuropharmacological perspectives. *Neurochem. Res.* 20:521–532.

Qiu, X.Q., K.S. Jakes, P.K. Kienker, A. Finkelstein, and S.L. Slatin. 1996. Major transmembrane movement associated with colicin Ia channel gating. *J. Gen. Physiol.* 107:313–328.

Repke, H., and M. Bienert. 1987. Mast cell activation—a receptor-independent mode of substance *P* action? *FEBS Lett.* 221:236–241.

Repke, H., W. Piotrowski, M. Bienert, and J.C. Foreman. 1987. Histamine release induced by Arg-Pro-Lys-Pro$(CH_2)_{11}CH_3$ from rat peritoneal mast cells. *J. Pharmacol. Exp. Ther.* 243:317–321.

Sayama, S., R.V. Iozzo, G.S. Lazarus, and N.M. Chechter. 1987. Human skin chymotrypsin-like proteinase chymase. *J. Biol. Chem.* 262:6808–6815.

Sigworth, F.J., H. Affolter, and E. Neher. 1995. Design of the EPC-9, a computer-controlled patch-clamp amplifier. 2. Software. *J. Neurosci. Methods.* 56:203–215.

Tso, J.Y., X.H. Sun, T.-H. Kao, K.S. Reece, and R. Wu. 1985. Isolation and characterization of rat and human glyceraldehyde-3-phosphate dehydrogenase cDNAs: genomic complexity and molecular evolution of the gene. *Nucleic Acids Res.* 13:2485–2491.

Vitale, N., M. Gensse, S. Chasserot-Golaz, D. Aunis, and M.F. Bader. 1996. Trimeric G-proteins control regulated exocytosis in bovine chromaffin cells: sequential involvement of G_o associated with secretory granules and G_{i3} bound to the plasma membrane. *Eur. J. Neurosci.* 8:1275–1285.

Vivès, E., P. Brodin, and B. Lebleu. 1997. A truncated HIV-1 Tat protein basic domain rapidly translocates through the plasma membrane and accumulates in the cell nucleus. *J. Biol. Chem.* 27: 16010–16017.

Winkler, A., G. Papsdorf, J. Odarjuk, W.-E. Siems, F. Fickel, and M.F. Melzig. 1995. Expression and characterization of the substance *P* (NK_1) receptor in the rat pituitary and AtT20 mouse pituitary tumor cells. *Eur. J. Pharmacol.* 291:51–55.

Yokota, Y., K. Sasai, T. Tanaka, K. Tsuchida, R. Shigemoto, A. Kakizuka, H. Ohkubo, and S. Nakanishi. 1989. Molecular characterization of a functional cDNA for rat substance *P* receptor. *J. Biol. Chem.* 264:17649–17654.

Published November 1, 1998